A Novel Metaheuristic Optimization for Throughput Maximization in Energy Harvesting Cognitive Radio Network

Shalley Bakshi*, Surbhi Sharma, Rajesh Khanna
Department of Electronics and Communication Engineering,
Thapar Institute of Engineering and Technology,
Patiala, Punjab, India
sbakshi60_phd19@thapar.edu

***Abstract*—In this article, a novel technique is proposed, namely rank-based multi-objective antlion optimization (RMOALO), and applied to optimize the performance of the energy harvesting cognitive radio network (EHCRN). The original selection method in multi-objective antlion optimizer (MOALO) is suitably changed to improve the algorithm, thus reaching the optimal solution for the problem. The proposed technique shows considerable performance improvement over the method used in the multi-objective antlion optimizer (MOALO). The performance of the proposed RMOALO is demonstrated on five benchmark mathematical functions and compared to multi-objective particle swarm optimization (MOPSO), multi-objective moth flame optimization (MOMFO), MOALO-Tournament, and MOALO-Roulette. The simulation results show an improved convergence of RMOALO and find the optimal solution to the throughput maximization problem. We show that RMOALO provides 16.33 % improved average throughput with the optimal value of sensing duration for the varying amount of harvested energy compared to MOPSO, MOMFO, MOALO-Roulette, and MOALO-Tournament.**

***Index Terms*—Cognitive radio; Energy harvesting; Metaheuristic optimization; MOALO; Spectrum sensing.**

I. INTRODUCTION

The demand and popularity of efficient wireless networks have increased over the past decade. Cognitive radio (CR) has been shown to be an emerging technology in wireless networks [1]. Cognitive radios are battery-operated with a limited network lifetime [2], [3]. With the advent of new devices, the efficient use of spectrum and energy has become a concern for most researchers. Energy harvesting is a promising addition to cognitive radio networks (CRN) to save energy and maximize throughput in next-generation wireless networks [4]. Energy harvesting is achieved from different energy sources in an energy harvesting cognitive radio network (EHCRN). The sources of energy in [5] are ambient such as solar, wind, motion, etc. from where the energy is harvested. The cognitive radio system uses ambient energy sources in [6], [7]. The RF (radio frequency) signal utilized by the secondary network acts as a source depending on the state of the channel in [8].

To meet the aforementioned challenges, optimization of the parameters that affect the performance of the energy harvesting cognitive radio network is considered [9]. To efficiently utilize the energy harvesting from the primary transmitter (PT), both energy harvesting and information transfer can be accomplished using the separated spectrum sensing and energy harvesting scheme (SSSEH). It can improve wireless network throughput, sensing time, and reduce the risk of collision between the primary transmitter and the primary receiver.

Manuscript received 11 December, 2021; accepted 23 May, 2022.

II. RELATED WORKS

For the EHCRN in [10], the average throughput of the secondary network is maximized by an optimal pairing of the sensing duration and the energy detector sensing threshold. In [11], a hidden Markov model describes the imperfect spectrum sensing process. The network obtains the optimal solution while adapting its parameters based on quality of service (QoS) requirements [12]. Some previous works have maximized throughput by optimizing resource allocation between primary and secondary users [13]. To maximize the throughput of the secondary user, optimal spectrum sensing energy, the transmit energy, and spectrum sensing interval Markov decision process (MDP) framework is used in [14]. In [15], optimized sensing time is achieved to improve the throughput in CR with a trade-off between the two. The optimization problem solved in [16] with the energy constraint and the collision constraint maximizes the total throughput of the secondary network in which the ambient source has been used for harvesting. Optimization of sensing threshold and sensing duration jointly for throughput maximization of a CRN is studied in [17]. The throughput of CRN is maximized by maintaining a proper trade-off between the harvested energy and the transmission of data with an optimal transmission time for primary and secondary users in [18]. In [19], the harvesting interval and the transmission interval are optimized to maximize the total achievable throughput of cognitive radio networks to obtain the maximum total achievable throughput. The sensing interval problem of the idle and busy channels in the EH-based CR network was formulated in [20]. A Markov chain was developed to find the energy state transition probability to solve the energy wastage problem.

From the literature, it is seen that spectrum sensing

optimization has been extensively studied, and most of the researchers emphasized optimizing the trade-off for spectrum sensing and throughput in EHCRN by solving it as a convex optimization problem [18]–[20].

Despite the advances mentioned above, there is still a trade-off between throughput and sensing in EHCRN with constraints on interference and energy [21]. For example, the CR needs to sense the spectrum with the minimum energy in less time to get overall maximum throughput. These problems are solved using classical optimization techniques. These existing optimization methods incorporate high complexity if the problem has a trade-off and multiple parameters to be handled simultaneously. Constrained optimization problems are more challenging to solve than unconstrained optimization. Such constraints and trade-offs can be dealt with using metaheuristic-based multi-objective optimization, as it provides an optimal solution by optimizing two or more objectives simultaneously. Moreover, these techniques offer faster convergence and provide global solutions efficiently. Although in the literature [22], the issues of efficient resource utilization are solved using dynamic programming or mixed-integer non-linear programming (MNLP) but with a high computational cost.

For cognitive radio network (CRN), up to the authors knowledge, metaheuristic-based multi-objective optimization methods have been used in related topics in [23]–[25] and have given satisfactory results, but we are not sure about separated spectrum sensing and energy harvesting scenario (SSSEH) in energy harvesting cognitive radio networks where energy harvesting and spectrum sensing occur separately in particular. Motivated by the works mentioned above, the focus of our work is to improve the performance of an energy harvesting cognitive radio network with the maximum throughput requirement while satisfying energy and interference constraints. This is achieved by multi-objective optimization of the EHCRN using the proposed novel metaheuristic technique. Constrained optimization can be a great solution to existing spectrum and energy problems. Analytical expressions for throughput and energy ratio are developed under the separated spectrum sensing and energy harvesting (SSSEH) scenario. The performance comparison of throughput under parameters similar to the baseline technique proposed in [26] is made. The impact of interference, signal-to-noise ratio (SNR), and harvested energy on throughput is also studied.

We have implemented the optimization problem of throughput maximization using multi-objective particle swarm optimization (MOPSO) [27], multi-objective moth flame optimization (MOMFO) [28], multi-objective antlion optimization (MOALO)-Roulette and MAOLO-Tournament [29] in the separated spectrum sensing and energy harvesting (SSSEH) scenario. These optimization techniques lack the proper trade-off between their intensification and diversification processes and get stuck to the best local solution.

Thus, we propose a rank-based multi-objective antlion optimization algorithm (RMOALO), which can prevent the solution from getting stuck in the local optimum to find the global optimal sensing time, maximizing the average throughput. Additionally, RMOALO is tested for various benchmark functions to validate its effectiveness. Apart from this, the performance comparison of the proposed algorithm with other metaheuristic algorithms shows that RMOALO outperforms in reaching the optimal solution. The comparison helps to find the best suitable algorithm for the given problem. The key contributions of this research work are summarized as follows:

1. Formulation of throughput maximization as a non-convex optimization problem using the novel fitness function for average throughput in separated spectrum sensing and energy harvesting (SSSEH) scenario.
2. An improved rank-based multi-objective metaheuristic optimization algorithm is proposed and used to find an efficient global solution. The benchmarking of the proposed algorithm with the state-of-the-art metaheuristic algorithms is also done.
3. The simulated results compared with the conventional scheme demonstrate that the proposed metaheuristic algorithm substantially increases the throughput of the secondary transmitter (ST).

The rest of the paper is organized as follows. Section III introduces the system model of the separated spectrum sensing and energy harvesting scheme (SSSEH) in EHCRN. For the network's maximum throughput demand, the multi-objective optimization problem for throughput maximization is formulated in Section IV. A novel multi-objective algorithm is proposed to obtain the optimal sensing duration in Section V. Section VI presents the simulated results and discussions. Section VII concludes the paper and presents future work.

III. SYSTEM MODEL

The system model of CR equipped with wireless energy harvesting for separated spectrum sensing and energy harvesting (SSSEH) is illustrated in Fig. 1.

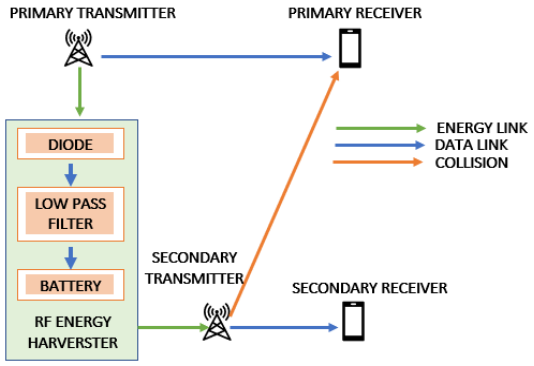

Fig. 1. Energy harvesting cognitive radio system for separated energy harvesting and spectrum sensing.

It consists of a primary and secondary network. The primary network consists of the primary transmitter-receiver pair and the secondary network consists of a secondary transmitter-receiver pair. The secondary transmitter (ST) is equipped with an RF energy harvester consisting of a rectifier unit and a rechargeable battery. The ST uses *harvest-store-use* for guaranteed QoS [30]. The primary network uses a licensed spectrum and has a fixed power source. Primary transmitter and receiver use synchronous slotted communication with the duration of the slot "*T*". The

secondary network is not licensed to use the spectrum, but opportunistically accesses the licensed user's spectrum depending upon the availability of the primary user. The ST senses the spectrum periodically according to the spectrum state of (H_0 or H_1) to harvest energy, signal sensing, and data transmission. H_0 gives the primary receiver state as an idle spectrum state and H_1 as an occupied spectrum state. The frame structure of SSSEH is illustrated using Fig. 2 [31].

1. Energy harvesting: In the interval (0, $\boldsymbol{\tau}_1$), if the primary transmitter is present, the energy harvester at the ST harvests from the RF signal of PT. The energy harvested is stored in the battery for future use. If the primary transmitter is absent, the energy harvester at ST stops as no RF signal will be present. In the absence of PT, harvesting is not done. The secondary transmitter is OFF during this time interval, i.e., there is no transmission in this phase. The ST works in the next phase using the stored energy, as there will be no RF energy due to the absence of PT.
2. Spectrum sensing: In the time slot ($\boldsymbol{\tau}_1$, $\boldsymbol{\tau}_2$), the energy harvester at the secondary transmitter stops harvesting and senses the spectrum. Spectrum sensing is performed with the energy of the storage device.
3. Data transmission: In the time slot (T - $\boldsymbol{\tau}_1$- $\boldsymbol{\tau}_2$), if the primary user is not detected, the sensing stops, and the data transmission occurs using the stored energy. During the data transmission slot, it becomes crucial to avoid collisions due to traffic between the primary transmitter-receiver pair. So, the energy and collision constraints are considered.

TABLE I. PRINCIPAL SYMBOLS' GLOSSARY.

τ_1	Energy harvesting time	σ^2_w	Noise Variance
τ_2	Sensing duration	σ^2_p	Signal Variance
T	Total frame period	P_{nc}	Probability of signal transmission without collision
$S(m)$	Primary transmitter signal	P_c	Probability of signal transmission with collision
$W(m)$	Noise signal	R_s	Average throughput at secondary
P_h	Energy arrival Rate	P_{tc}	Target Collison probability
E_h	Average energy harvested at harvester	E_{st}	Average energy at secondary
E_s	Energy consumed for sensing by secondary transmitter	P_s	Sensing probability
e_s	Sensing power	lb	Lower Bound
E_t	Energy consumed for transmission at the secondary transmitter	ub	Upper Bound
e_t	Data Transmit power	i	Number of iterations
θ_n	Channel status idle/occupied	Ant_i^t	The fitness value of the ant (i - position with t - iteration)
E_c	Total energy consumption	C_i^t	The minimum value of variables for the ant at i-th position
P_f	False alarm (probability)	d_i^t	This represents the maximum value of variables for the ant at i-th position
P_d	Detection (probability)		

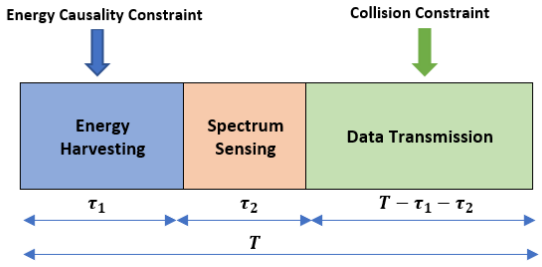

Fig. 2. The frame structure of separated energy harvesting and spectrum sensing.

IV. PROBLEM FORMULATION FOR MULTI-OBJECTIVE OPTIMIZATION

This section aims to formulate a fitness function for throughput maximization and the energy ratio at the secondary transmitter (ST).

A. Energy Harvesting and Consumption

The energy harvester in the secondary transmitter harvests energy from the RF signal of the primary transmitter if there is no user signal. As shown in Fig. 2, each frame duration is "T" and the energy arrival is random, with P_h as the average rate. In the harvesting slot, the average harvested energy is given as $E_h = P_h\tau_1$, which is available to the ST in the sensing slot. The secondary transmitter executes spectrum sensing operation using energy detection and consuming energy $E_s = e_s\tau_2$ in the sensing phase, where e_s is the power required for spectrum sensing. The assumption made in this model is that the energy harvested in different harvesting timeslots is not dependent on the channel between the primary transmitter and the RF energy harvester.

The Markov process is used to model the state occupation of the channel [32]. The sensing results of the channel being occupied or idle are given by the channel occupation state as $\theta_n \in \{0$ (idle), 1 (occupied)$\}$ for the slot n. The state transition probabilities with the channel occupancy state are illustrated in Fig. 3.

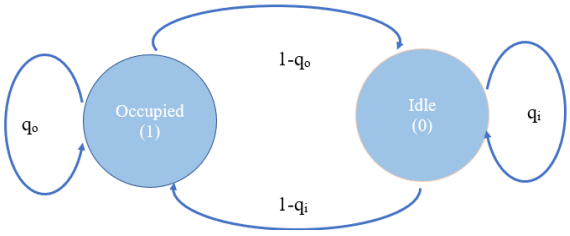

Fig. 3. State transition diagram.

Here, the probability of transit is q_i for the idle state and q_o for the occupied state. Thus, the steady-state probabilities are given by $\pi_i = \frac{1-q_o}{2-q_i-q_o}$ and $\pi_0 = \frac{1-q_i}{2-q_i-q_o}$, respectively [17], with $\boldsymbol{\pi_i + \pi_0 = 1}$.

Let e_t represent the power required for data transmission. If the secondary transmitter finds the spectrum occupied, i.e., $\theta_n = 1$, it starts harvesting the energy from the primary transmitter but does not consume energy for data transmission. If the channel is idle, i.e., $\theta_n = 0$, the secondary transmitter consumes $E_t = e_t(T - \tau_1 - \tau_2)(1 - \theta_n)$ energy during the transmission phase. Thus, the expression for the average energy consumed in slot n at ST is

$$E_c = [e_s\tau_2 + e_t(T-\tau_1-\tau_2)(1-\theta_n)]. \quad (1)$$

Energy consumption should not exceed the amount of harvested energy, i.e., $E_c \le E_h$, in each slot, since the harvested energy depends on the availability of the primary transmitter signal, so the energy constraint is considered to meet the power required for sensing and transmission.

When the secondary transmitter is active and the primary channel is idle, the novel fitness function derived from the energy ratio in terms of the average energy harvested into the average energy consumption is given as

$$E_{ratio} = \frac{P_h\tau_1}{[e_s\tau_2 + e_t(T-\tau_1-\tau_2)(1-\theta_n)]}, \quad E_c \le E_h. \quad (2)$$

Energy consumption and spectrum sensing are intertwined, since ST consumes energy during the sensing phase. So, it becomes essential to consider the restrictions on energy consumption for sensing in the separated spectrum sensing and energy harvesting (SSSEH).

B. Optimization of Sensing Duration for Throughput Maximization

Spectrum sensing is performed by the secondary transmitter with energy detection of the RF signal periodically in the duration of the slot "*T*". It is also assumed that the secondary transmitter has enough data for transmission. The following hypothesis is considered to detect whether the spectrum is occupied or idle

$$y_n(m) = \begin{cases} w(m), H_0, \\ s(m) + w(m), H_1, \end{cases} \quad (3)$$

where H_0 and H_1 give the channel state (occupied or idle), respectively, $y_n(m)$ is the m^{th} sample of the energy detector in a slot "*n*", *s(m)* represents the signal of the primary transmitter, and *w(m)* represents the noise, respectively. Both are random processes that are supposed to be independent circularly symmetric complex Gaussian (CSCG) with respective variances σ^2_p and σ^2_w. To optimize the sensing duration τ_2 in the SSSEH scenario, the sensing performance is given in terms of the false alarm probability $P_f(\boldsymbol{\tau_2}, \boldsymbol{\varepsilon})$, and signal detection probability $P_d(\boldsymbol{\tau_2}, \boldsymbol{\varepsilon})$:

$$P_f(\tau_2, \varepsilon) = Q\left(\left(\frac{\varepsilon}{\sigma_w^2} - 1\right)\sqrt{\tau_2 f_s}\right), \quad (4)$$

$$P_d(\tau_2, \varepsilon) = Q\left(\left(\frac{\varepsilon}{\sigma_w^2 + \sigma_p^2} - 1\right)\sqrt{\tau_2 f_s}\right), \quad (5)$$

where Q(x) represents the standard q function, $\varepsilon \in$ R+ represents the threshold where R+ denotes the set of non-negative real numbers, and f_s represents the sampling frequency. The number of samples in the sensing slot is $\tau_2 f_s$. As the secondary transmitter harvests the RF energy from the primary transmitter, there is a likelihood of collision between the primary and secondary transmitters.

Case I Primary network is idle. Let $P_{nc}(\tau_2, \varepsilon, P_h)$ denote the probability of no collision while sensing when the primary channel used by the primary network is idle. The throughput of the secondary network when the primary network is idle is $R_{nc} = \log(1+\gamma_s)$, where γ_s is signal-to-noise ratio at the input of the secondary transmitter

$$P_{nc}(\tau_2, \varepsilon, P_h) = P_s(\tau_2, \varepsilon, P_h)(1 - P_f(\tau_2, \varepsilon)), \quad (6)$$

where $P_s(\tau_2, \varepsilon, P_h)$ is the probability of the secondary transmitter being active. The system is considered active from a long-term perception. There is an upper bound on the activation probability in SSSEH given by

$$P_s(\tau_2, \varepsilon, P_h) \le \bar{P}_s(\tau_2, \varepsilon, P_h) = \\ = min(1, Est(\tau_1, \tau_2, \varepsilon, P_h)). \quad (7)$$

Case II Primary network is occupied. Let $P_c(\tau_2, \varepsilon, P_h)$ denote the probability of collision while sensing when the primary channel is occupied. The throughput of the secondary network when the channel is occupied is $R_c = \log(1 + \frac{\gamma_s}{(1+\gamma_p)})$. The received signal-to-noise ratio in the secondary network for secondary and primary signals is γ_s and γ_p, respectively

$$P_c(\tau_2, \varepsilon, P_h) = P_s(\tau_2, \varepsilon, P_h)(1 - P_d(\tau_2, \varepsilon)). \quad (8)$$

The average throughput of the ST depends on the probability that the secondary transmitter transmits without collision and in the presence of collision. Thus, the normalized average throughput R_s using (6) and (7) is given as

$$R_s(\tau_1, \tau_2, \varepsilon, P_h) = \frac{(T-\tau_1-\tau_2)}{T}[(P_{nc}(\tau_2, \varepsilon, P_h)\pi_o C_i + \\ + P_c(\tau_2, \varepsilon, P_h)\pi_i C_o)]. \quad (9)$$

Protection of the licensed user, i.e., the primary receiver, is of utmost importance. So, when the channel of the primary network is occupied, the collision probability should be less than its target value

$$P_c(\tau_2, \varepsilon, P_h) \le P_{tc}, \quad (10)$$

where $\boldsymbol{P_{tc}}$ is the target collision probability of protecting the primary network. Here, the sensing duration is a crucial term to which throughput maximization is achieved. Therefore, the novel fitness function used for sensing duration optimization is formulated as

$$\begin{aligned} &\max_{\tau_2} R_s(\tau_1, \tau_2, \varepsilon, P_h), \\ &s.t\ P_c(\tau_2, \varepsilon, P_h) \le P_{tc}, E_c \le E_h. \end{aligned} \quad (11)$$

To maximize the fitness function in (11), the rank-based multi-objective optimization (RMOALO) is proposed to optimize the sensing duation and solve the problem of throughput maximization in the given optimization problem.

V. PROPOSED META-HEURISTIC ALGORITHM (RMOALO) AND OTHER TECHNIQUES TO SOLVE SENSING DURATION OPTIMIZATION PROBLEM IN SSSEH

We use multi-objective optimization algorithms to solve the constrained optimization problem with multiple variables. In particular, MOPSO, MOMFO, MOALO, and the proposed RMOALO are used to solve duration optimization problem for the sensing. A brief description of these algorithms is given below.

A. Multi-Objective Particle Swarm Optimization

MOPSO [27] extends particle swarm optimization (PSO) to handle multiple objectives. Multi-objective particle swarm optimization incorporates Pareto dominance into PSO. This concept creates preferences among the swarm particles, developing leaders and guiding other particles. These different leaders are the solutions, but only one leader is selected to update the velocity that represents their movement.

MOPSO involves the basic steps:

– Initialization of the population of particles "*i*" as *pop[i]* and the velocity of each particle *vel[i]*. Each particle "*i*" has a position *pop[i]* ∈ *rep*, representing a possible solution. After a certain time, the position of the particle is obtained by adding its velocity, *vel[i]* ∈ *rep*, to *pop[i]*

$$pop[i] = pop[i] + vel[i]. \tag{12}$$

– Evaluate each of the particles in the population and store the position of the particles in the population representing non-dominated solutions and leaders in the repository (*rep*).

– Initialize the memory of each particle that guides it to travel through the search space. This memory is also stored in the repository.

– The velocity of a particle "*i"* is based on the best position already fetched by the particle, *pbest[i]*, and the best position already fetched by the set of neighbors of "*i*", *rep*, which is a leader of the repository

$$vel[i] = IW \times vel[i] + r_1 \times (pbest[i] - pop[i]) + r_2 \times \times (rep[h] - pop[i]). \tag{13}$$

The coefficient *IW* is the particle inertia that controls how much the previous velocity affects the current one and takes a value of 0.4; r_1 and r_2 are random numbers in the range [0…1]. If the new position and the current *pbest[i]* are non-dominated, the new value is chosen randomly between these two vectors. *rep[h]* is a particle from the repository, chosen as a guide for *i*.

As there are many best solutions from which the fittest one should be chosen, but due to lack of exploitation, MOPSO is incapable of searching globally. Therefore, it converges early without finding the fittest solution. Hence, we tend to solve the problem with the MOMFO algorithm.

B. Multi-Objective Moth Flame Optimization

MOMFO has modified Moth flame optimization [33] that includes the following steps.

– Initialize the position of "i" number of "m" moths and "j" number of "f" flames.

– For each moth position, evaluate fitness.

– Store the non-dominated solutions in the repository storage, i.e., positions of the moth.

– Find the best local position for each moth in the first iteration, update the moth position in the second iteration onwards, and compare the updated position of moth with the previous position.

– The position of each moth "i" is updated with respect to j^{th} flame

$$m_i = S(m_i, f_j), \tag{14}$$

where *S* designates a spiral function which permits each moth to fly around a flame; it is not clear that the moth has to fly in the space between the moth position and the flame. It can also discover the other space. Therefore, there is a more efficient exploration and exploitation of the search space by moths

$$S(m_i, f_j) = d_i e^{bt} \cos 2\pi t + f_j, \tag{15}$$

where d_i is the absolute distance $|f_j - m_i|$, *b* is the constant for controlling the shape of the logarithmic spiral function, *t* is a random number between [-1, 1]. Furthermore, the reduction in number of flames N_f is adaptive and is reduced with respect to the increase in iteration

$$N_f = round\left(Niter_{f\max}\right)\left(\frac{N_{f\max}}{I_{maxiter}}\right), \tag{16}$$

where N_{fmax} is the maximum number of flames. The MOMFO has the capability to reach the best solution due to efficient exploration and exploitation of the search space as this algorithm updates the position based upon the absolute distance between moth and flame.

C. Multi-Objective Antlion Optimizer (MOALO)

MOALO is the extended version of Antlion Optimization (ALO) and follows the same search behavior as ALO. It is inspired by the unique hunting behavior of antlions. Antlions are net-winged insects, and the chosen prey are ants. Antlions form the cone-shaped trap in the sand for ants while throwing out the sand [34].

Mathematical Modeling of MOALO. The mathematical modeling of hunting includes five different steps: search agents with random walk, trap formation, trap ants, catching prey, trap reconstruction, and elitism [35].

Random walk of search agents. The search for food makes the ants move stochastically over the search space. The hunting process of antlions is modeled by the interaction of the antlions with the ants modeled by random walk as

$$X(t) = [0, cumsum(2r(t_1) - 1), cumsum(2r(t_2) - -1)\ldots\ldots, cumsum(2r(t_{\max - iter}) - 1)]. \tag{17}$$

The cumulative sum is calculated by cumsum with the maximum number of iterations as *max-iter* and ***r*(*t*)** as a stochastic function, and *t* indicates the random walk step, and the rand is any number between 0 and 1

$$r(t)=\begin{cases}1\ if & rand>0.5,\\ 0\ if & rand\le 0.5.\end{cases} \quad (18)$$

The steps of the ant should be within defined boundaries, so

$$X_i^t=\frac{(X_i^t-a_i)\times(d_i^t-C_i^t)}{(b_i-a_i)}+C_i^t, \quad (19)$$

where a_i and b_i signify the *i-th* ant variable showing the minimum and maximum random walk. For each iteration, C_i^t and d_i^t represent the *i-th* variable indicating the minimum and maximum at the iteration *t*, respectively.

Trap ants. The random walk of ants is affected by the hypersphere traps represented by vectors *c* and *d* set by the Antlions:

$$c_i^t=Antlion_j^t+c^t, \quad (20)$$

$$d_i^t=Antlion_j^t+d^t, \quad (21)$$

where c^t and d^t are the minimum and maximum of all the variables in the *t-th* iteration, $Antlion_j^t$ at the *t-th* iteration represents the position of the selected *j-th* antlion.

Sliding ants towards antlions. The ants slid towards antlions by shooting the sand outwards by them. The trapped ants slide down, thus preventing them from escaping. Hence, reducing the boundaries of the random walk of the ant to get a decreasing radius of the hypersphere is modeled as:

$$c^t=\frac{c^t}{I}, \quad (22)$$

$$d^t=\frac{d^t}{I}, \quad (23)$$

where *I* is a ratio for controlling the radius, c^t and d^t is the minimum and maximum of all the variables at the *t-th* iteration.

The ratio $I=1+10^w\frac{t}{T}$, where *t* represents the current iteration, *T* is the maximum number of iterations, and *w* is defined based on the current iteration.

Catching prey and reconstruction of the pit. The prey caught (ant) at the bottom of the pit becomes fitter than its corresponding antlion. An antlion is then required to update its position to the latest position of the hunted ant to catch new prey in the next iterations. The following equation simulates this

$$Antlion_j^t=Ant_i^t \quad if \quad f(Ant_i^t)\prec f(Antlion_j^t). \quad (24)$$

Here, *t* denotes the current iteration and Ant_i^t specifies the *i-th* position of the ant at iteration *t*. The function *f* denotes the fitness value, and $\prec$ shows the Ant_i^t rules $Antlion_j^t$.

Elitism. Maintaining and saving the fittest antlion obtained at any point of the optimization process depends on the concentration of solutions in the search space and is known as elitism. The elite antlion is the fittest antlion in each iteration

$$Ant_i^t=\frac{R_A^t+R_E^t}{2}, \quad (25)$$

where R_A^t is the random walk around the antlion in iteration *t*, and R_E^t is the random walk around the elite in iteration *t*. Here, the roulette wheel is used to select the random walk.

The archive is updated with the solutions explored in the next iteration. The selected solution is based on the probability using the equation as follows

$$P_i=\frac{c}{N_i}. \quad (26)$$

The probability with which the solution is removed from the archive is as follows

$$P_i=\frac{N_i}{c}. \quad (27)$$

Here, N_i represents the number of solutions for the *i*-th solution in the neighborhood, and *c* is a constant with a value greater than 1.

As MOALO gives diverse new solutions having very close values, it is necessary to handle this behavior with a suitable algorithm.

D. Proposed Novel Rank-based Multi-Objective Antlion Optimization (RMOALO)

The strength of a metaheuristic algorithm on a given optimization problem is determined by its ability to provide a balance between the global search and the local search. The proposed algorithm (see Algorithm 1) uses rank-based selection instead of the roulette wheel selection used in MOALO. To prove the competence of this selection method, we have also implemented MOALO with a tournament-based selection method. Tournament selection is used in one of the variants of antlion optimization (ALO) [36]. MOALO uses a repository to store non-dominated Pareto optimal solutions obtained at a given point in time. Solutions are then chosen from this repository using a roulette wheel mechanism based on the coverage of solutions as antlions to guide ants towards promising regions of multi-objective search spaces. The selection probability of all individuals becomes almost identical, which works against the basic idea of genetic algorithms. Thus, we proposed the algorithm, which is named a "rank-based multi-objective optimization algorithm" (RMOALO). Rank-based selection involves sorting all the random walks in decreasing order, arranging them in a queue, and moving towards the antlions from the higher-order rank to the lower one. Therefore, the position of ants in (25) updated using a roulette wheel is modified to rank selection, helping to faster convergence. Thus, the arrangement of random walk of ants is listed in decreasing order and ranked accordingly followed by the rank of ants:

$$p_1^{t-1}\ge p_2^{t-1}\ge p_3^{t-1}\ldots\ldots\ldots p_n^{t-1}, \quad (28)$$

$$R_y^t \forall \in [R_1^t, R_2^t, R_3^t .....R_n^t]. \quad (29)$$

Algorithm 1. Pseudocode of the RMOALO algorithm.

```
1. Initialize ant (potential solutions) of
    normalized sensing period (x ϵ (0,1)) with
    population size N, and max number of
    iterations.
2. Assign the value for parameters T, Es, Et,
    Eh, N (for which algorithm needs to be
    executed).
3. Calculate Fitness value, i.e., Average
    Throughput function for each solution from
    step 1. Fittest
4. Select Antlion using Rank. Update its
    respective position (elite antlion).
5. While (iteration count is less than max
    iteration)
    for (Each antlion)
       Antlion to be selected by rank
       selection method.
       Randomly walking ants are slided in to
       the trap as per following criteria:
       opt=rand;
              if opt > 0.75
              lb=antlion+lb;
              ub=antlion+ub;
              elseif opt > 0.5
              lb=antlion-lb;
              ub=antlion-ub;
              elseif opt > 0.25
              lb=-antlion+lb;
              ub=-antlion+ub;
              else
              lb=-antlion-lb;
              ub=-antlion-ub;
              end
       Generate random walk of Ant's path
       around elite antlion
       Generate random walk of Ant's path
       around the shortlisted antlion
       Normalize random walk and compute the
       location of Ant
       if Ant is available in the search
       dimension.
          Make the ant relocate in search
          dimension
       end if
    end for
    fitness factor of ants needs to be
    calculated
    for (each antlion)
       if the fitness factor is improved
       compared to antlion
           antlion eats up Ant (antlion needs
           to be updated)
       end if
    end for
    Update the elite antlion

End while
```

The updated position of the ants after ranking is given by

$$Ant_i^t = \frac{R_y^t + R_E^t}{2}, \quad (30)$$

where $y \forall \in [1, 2, ..., n]$.

Mapping Metaheuristics to Throughput Maximization in SSSEH. Relating the metaheuristic technique to the fitness function is essential for understanding the behavior of the problem and solution. Similarly to the mapping done between the algorithm based on swarm intelligence and energy-efficient CR in [37], the correlation between the metaheuristic algorithms and the fitness function becomes important (see the data in Table II below).

TABLE II. METAHEURISTIC ALGORITHMS AND FITNESS FUNCTION ANALOGY.

S. no.	Throughput Function	MOPSO	MOMFO	MOALO/ RMOALO
1	Decision Variables Count	Swarm Behavior	Moth and flame characteristics	Ant characteristics
2	Secondary transmitter-Sensed samples	Number of particles/swarm	Number of moth and flame	Number of ants/search agents
3	Fitness function-Throughput maximization	Fitness value of swarm	Fitness of Moth position	Fitness value of Ant
4	Optimum solution-Sensing duration	Fittest particle position	Position of the moth based upon distance to flame	Elite Antlion position and its fitness value

VI. SIMULATION RESULTS AND DISCUSSION

In this section, the throughput analysis for the separated spectrum sensing and energy harvesting scenario for the EHCRN with the proposed algorithm is confirmed by means of MATLAB simulations. The implementation was performed on a machine running the Windows 10 operating system version 21H1. It has an installed RAM of 8 GB using 11th Gen Intel(R) Core(TM) i5-1135G7 @ 2.40 GHz 1.38 GHz, 64 Bit Processor. For simulation purposes, the system parameters used are mainly derived from [14] (as shown in Table III below). The average harvested energy is taken between 0.01 μw to 0.16 μw [38].

TABLE III. PARAMETER VALUES.

Symbol	Parameter	Default Value
T	Duration of a timeslot	0.1 s
E_s	Sensing energy	110 mW
E_t	Data transmission energy	410 mW
E_h	Average harvested energy	0.01 μw to 0.16 μw
SNR	Signal-to-noise ratio	-15 dB
N	Number of sensing samples	1000

The simulation settings for all five algorithms are: population size is 20, number of iterations is 500, archive size is 100, and 30 Monte Carlo trials are performed for each case. The extremely large value of this population size (e.g., 90) will increase the computational complexity of the optimization algorithms, which is undesirable. So, an intermediate value of the population is chosen.

To measure the effectiveness of the proposed rank-based multi-objective antlion optimization (RMOALO), we have considered five different test functions F1–F5. The details of the benchmark functional parameters in terms of dimensionality, search domain, and optimal global value are shown in Table IV below [39], [40]. The dimensionality exhibits the dimensions of the test functions, and the search domain marks the test area of the search space, and the

global minimum showcases the minimum value taken by the test functions to achieve convergence.

The comparative performance of the proposed algorithm and other algorithms for different test functions is given using the mean minimum, maximum, and standard deviation metrics (see data in Table V).

TABLE IV. DIMENSIONALITY, SEARCH DOMAIN, AND GLOBAL MINIMA FOR DIFFERENT BENCHMARK FUNCTIONS.

Name	Function	Dimensionality	Search Domain	Global Minima
ZDT1 (F1)	$Minimize:\ f_1(x) = x_1$ $Minimize:\ f_2(x) = g(x) \times h(f_1(x), g(x)), where:$ $G(x) = 1 + \frac{9}{N-1}\sum_{i=2}^{N} x_i$ $F1(f_1(x), g(x)) = 1 - \sqrt{\frac{f_1(x)}{g(x)}}$ $0 \le x_i \le 1,\ 1 \le i \le 30$	2	[0, 1]	0
Ackley (F2)	$f(x) = -20exp[-0.2\sqrt{\frac{1}{D}\sum_{i=1}^{D} x_i^2}] - exp[\frac{1}{D}\sum_{i=1}^{D}\cos 2\pi x_i] + 20 + e$	30	[-100, 100]	0
EASOM (F3)	$f(x) = -cos(x_1)cos(x_2)exp[(x_1-\pi)^2 - (x_2-\pi)^2]$	2	[-100, 100]	-1
GRIEWANK (F4)	$f(x) = \sum_{i=1}^{D}\frac{x_i^2}{4000} - \prod_{i=1}^{D}\cos\frac{x_i}{\sqrt{i}} + 1$	30	[-600, 600]	0
RASTRIGIN (F5)	$f(x) = 10D + [\sum_{i=1}^{D} x_i^2 - 10\cos 2\pi x_i]$	30	[-5.12, 5.12]	0

TABLE V. PERFORMANCE COMPARISION OF MOMFO, MOPSO, MOALO-TOURNAMENT, MOALO-ROULETTE WHEEL, AND RMOALO FOR DIFFERENT TEST FUNCTIONS.

Test Function	Algorithm	Mean	Minimum	Maximum	Std Deviation
F1 ZDT1	**MOPSO**	0.4420415	0.0028335	1	0.274110095
	MOMFO	4.276522167	0.301349762	8.789737424	2.15542331
	MOALO-Roulette Wheel	0.695312479	0.509284203	1.009716235	0.157357799
	MOALO-Tournament	0.6765339	0.5700102	1.0000000	0.112807534
	Proposed RMOALO	0.777572714	0.692868283	1.002267562	**0.083223097**
F2 Ackley	**MOPSO**	16.437788	2.054921	21.06954613	5.510931771
	MOMFO	20.42244285	2.786300012	22.34790691	4.250018151
	MOALO-Roulette Wheel	15.84560452	0.000649989	19.97847592	6.201644477
	MOALO-Tournament	16.20895104	0.038137074	19.99663289	5.509201695
	Proposed RMOALO	16.18311188	0.829800307	20.30860279	**4.134937919**
F3 Easom	**MOPSO**	-1.75E-22	-6.12E-21	0.00E+00	1.03441E-21
	MOMFO	2.48E-07	-1.08E-23	2.48E-05	2.47965E-06
	MOALO-Roulette Wheel	-0.19307025	-0.885716657	-2.2144E-273	0.295860643
	MOALO-Tournament	-4.24E-04	-4.24E-02	-1.06E-272	0.004243454
	Proposed RMOALO	-9.12E-03	-4.56E-01	-1.56E-285	**0.053573036**
F4 Griewank	**MOPSO**	71.39511561	11.14875606	180.0120547	38.55836861
	MOMFO	35.68924762	1.299758186	91.13924973	20.76193545
	MOALO-Roulette Wheel	17.69652674	0.36676992	50.16619774	13.32720051
	MOALO-Tournament	11.84277996	0.21466434	50.11672004	10.69809831
	Proposed RMOALO	13.23507481	1.077900875	50.24496823	**10.38179246**
F5 Rastrin	**MOPSO**	32.8	4.072911	57.849427	15.2126232
	MOMFO	37.37558614	9.62931289	77.61343833	13.72352695
	MOALO-Roulette Wheel	31.01756762	9.370621181	53.47901187	11.50756297
	MOALO-Tournament	29.63183816	8.0510918	52.01330333	10.14598691
	Proposed RMOALO	16.34113611	4.287325569	62.38888473	**11.47344816**

Rank-based multi-objective optimization (RMOALO) shows the least standard deviation for the functions F1, F2, and F4 and is close to the lowest standard deviation for the rest of the two functions F3 and F5. On the other hand, Multi-objective moth flame optimization and multi-objective particle swarm optimization (MOPSO) have displayed relatively higher standard deviation for most of the functions. This clearly shows that rank-based multi-objective optimization has relatively high stability, thus showing robustness and consistency in its performance. Thus, it can be interpreted that the proposed RMOALO is superior or comparable to other algorithms. For any optimization algorithm, it is very important that it should not be stuck to the local optima and should converge faster.

The convergence characteristics for the benchmark test functions (F1–F5) for each algorithm are shown in Figs. 4–8 for SNR values −15 dB. In this paper, to get a clearer view on the dependency of the fitness function on each variable,

the convergence curve is plotted for the optimum value of each variable. The convergence of the proposed algorithm is much better than the other algorithms towards the optimum value of the fitness function. Because of the rank selection method, it is able to successfully overcome the local optima and find the global optima. RMOALO can reach an optimal value in fewer iterations, also avoiding premature convergence.We have evaluated the strength and competence of the proposed RMOALO and other algorithms by applying it to the sensing duration optimization problem to achieve maximum throughput for EHCRN. The fitness function in (11) is optimized for three different values of the harvested energies. Thirty independent runs are made to eliminate any inconsistency, involving 30 Monte Carlo initial trial solutions with a randomly generated population of size 20. The maximum number of iterations is set to 1000. The performance parameters of the formulated problem have been given in terms of the mean, maximum, median, and standard deviation values of the normalized sensing duration (ratio of the sensing duration to the overall time slot) along with the mean fitness value of average throughput (data in Table VI). RMOALO is observed to provide the higher value of throughput in various iterations of the harvested energy E_h at the lowest mean value of the normalized sensing duration. It is also stable in its performance, as it offers the lowest standard deviation among all other algorithms.

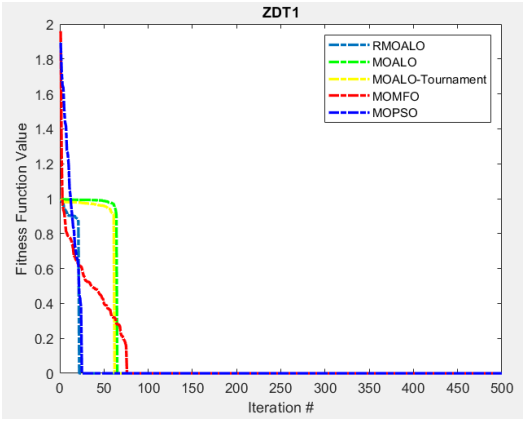

Fig. 4. Convergence characteristics for ZDT1.

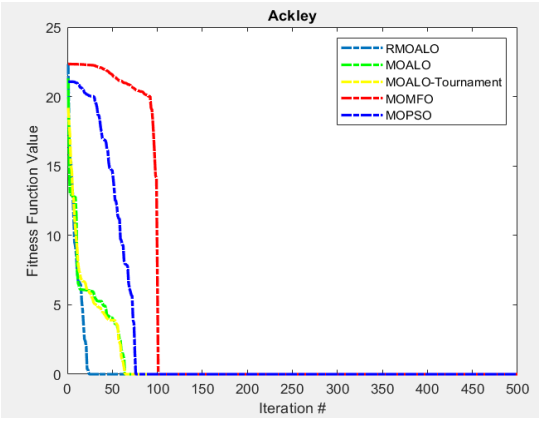

Fig. 5. Convergence characteristics for Ackley.

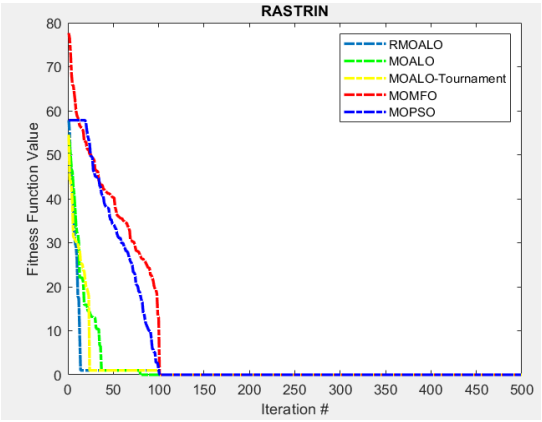

Fig. 6. Convergence characteristics for RASTRIN.

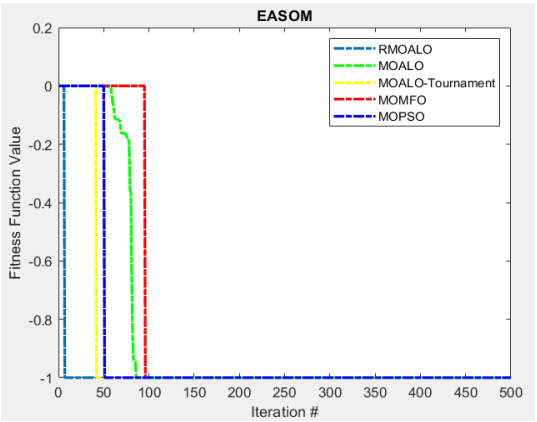

Fig. 7. Convergence characteristics for Easom.

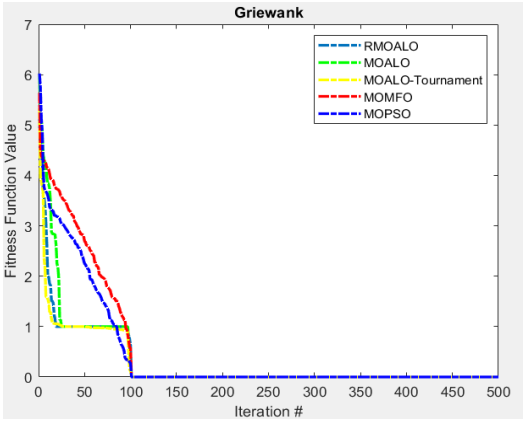

Fig. 8. Convergence characteristics for Griewank.

TABLE VI. COMPARISION OF STATISTICAL RESULTS OF NORMALIZED SENSING DURATION, AVERAGE THROUGHPUT FOR VARYING HARVESTED ENERGY.

	Normalized Sensing Duration				Average Throughput
ALGORITHM	**Mean**	**Maximum**	**Median**	**Standard Deviation**	**Mean fitness value**
			E_h = 0.13 µw		
MOPSO	0.47018	0.8	0.5046	0.210751497	0.534947943
MOMFO	0.436468	0.799919	0.4641	0.244203995	0.586831472
MOALO-Roulette Wheel	0.323484	0.8	0.2264	0.31343693	0.735205996
MOALO-Tournament	0.213435	0.8	0.185	0.161605791	0.946340244
Proposed RMOALO	**0.135812**	0.8	0.0883	**0.162575498**	**1.054686624**
			E_h = 0.10 µw		
MOPSO	0.418764	0.8	0.4651	0.252006978	0.560740295
MOMFO	0.3898	0.780895	0.2242	0.224243203	0.604630478
MOALO-Roulette Wheel	0.142679	0.8	0.2061	0.144568157	1.007506222
MOALO-Tournament	0.109786	0.794098	0.0605	0.13707374	1.07852165
Proposed RMOALO	**0.109754**	0.8	0.0861	**0.120687845**	**1.088715996**
			E_h = 0.07 µw		
MOPSO	0.359586	0.8	0.3503	0.242864035	0.48524242
MOMFO	0.389411	0.789658	0.3807	0.215096189	0.433160618
MOALO-Roulette Wheel	0.132189	0.8	0.0849	0.148451314	0.132189402
MOALO-Tournament	0.352831	0.8	0.3714	0.335657676	0.555828206
Proposed RMOALO	**0.089198485**	0.8	0.031852806	**0.141880092**	**0.893501103**

The convergence characteristics of the average throughput for different values of the average harvested energy (E_h) are shown in Figs. 9–11. The RMOALO has the ability to overcome local optima with better convergence and is successful in obtaining the best values as compared to other algorithms. The impact of normalized sensing duration on the average throughput with RMOALO reaches a maximum in a few iterations. Thus, RMOALO converges faster to get the higher fitness value.

We can see from Table VI that the behavior of the sensing duration changes with the average harvested energy in three distinct values of the harvested energy E_h = 0.13 µw, E_h = 0.10 µw, and E_h = 0.07 µw. The shorter the sensing duration, the higher the average throughput if the harvested energy is higher. As the normalized sensing duration increases, the average throughput tends to decrease. Therefore, an optimal value of sensing duration τ_2 exists for the amount of energy harvested for which the average throughput becomes maximum. For a particular sensing time, the average throughput decreases as E_h decreases. When E_h is maximum, the average throughput R_s attains a maximum value, and after reaching a maximum value, it decreases as there is an increase in τ_2 and decrease in E_h.

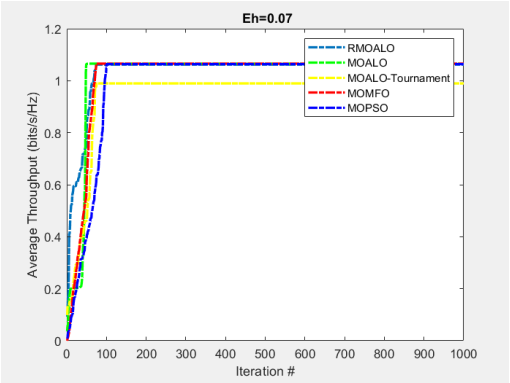

Fig. 9. Average throughput across iterations when the harvested energy Eh = 0.07 µw.

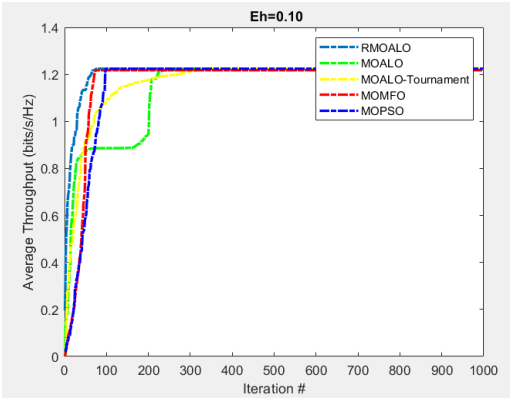

Fig. 10. Average throughput across iterations when the harvested energy Eh = 0.10 µw.

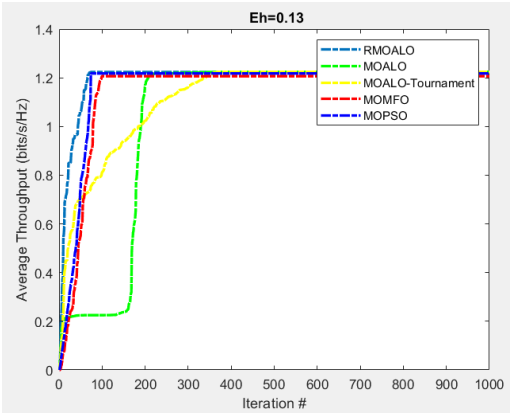

Fig. 11. Average throughput across iterations when the harvested energy Eh = 0.13 µw.

To validate the effectiveness of the proposed optimization technique, a comparison of throughput maximization for the separated spectrum sensing and energy harvesting (SSSEH) scenario is also done with baseline energy-efficient spectrum sensing schemes in the cognitive radio network. The same initial setup conditions of the sensing duration = 50 µs, average harvested energy E_h = 300 J, the sensing

energy E_s = 1 J, and the energy consumed for transmission E_t = 3 J are considered for simulation purposes. Figure 12 shows the analysis for SNR = −28 dB. The throughput achieved using RMOALO shows 14.02 % improvement over the energy-efficient spectrum-sensing scheme - homogeneous CR and 6.74 % improvement over the energy-efficient spectrum-sensing scheme - heterogeneous CR, as shown in Table VII.

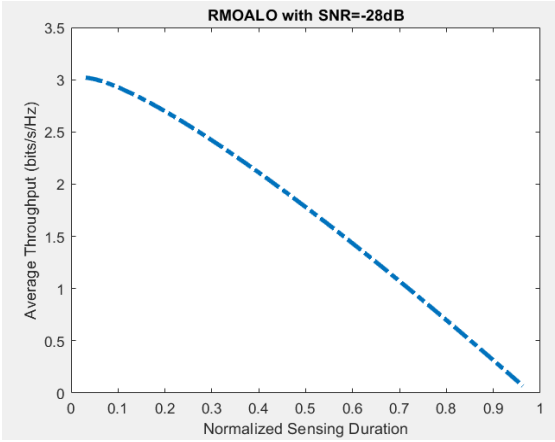

Fig. 12. Improvement in performance using RMOALO compared to the baseline scheme.

TABLE VII. AVERAGE THROUGHPUT VERSUS NORMALIZED SENSING DURATION.

Scheme	Maximum Throughput	Reference
Energy-efficient spectrum sensing scheme - homogeneous network	2.64	Table IV [26]
Energy-efficient spectrum sensing scheme - heterogeneous network	2.82	Table IV [26]
Separated spectrum sensing energy harvesting - EHCRN	3.01	Fig. 12

VII. CONCLUSIONS

In the separated spectrum sensing and energy harvesting cognitive radio network with the maximum throughput demands, we maximized the average throughput by optimizing the sensing duration of the ST. This has been achieved by leveraging the proposed RMOALO metaheuristic algorithm. With the SNR value of -15 dB and population size = 20, for varying the sensing time and the average harvested energy, the proposed RMOALO is 16.33 % more efficient than other metaheuristic algorithms considered.

There are several directions in which the analysis of this work could be extended. As the work considers EHCRN and metaheuristics, it can be extended from both realms for some future research, such as non-linear energy harvesting device-to-device network [41], hybrid metaheuristic optimization [42], and bidirectional networks [43].

CONFLICTS OF INTEREST

The authors declare that they have no conflicts of interest.

REFERENCES

[1] J. Mittola and G. Q. Maguire, “Cognitive radio: Making software radio more personal”, *IEEE Personal Communications*, vol. 6, no. 4, pp. 13–18, Aug. 1999. DOI: 10.1109/98.788210.

[2] E. F. Orumwense, T. J. Afullo, and V. M. Srivastava, “Achieving a better energy-efficient cognitive radio network”, *Int. J. Comput. Inf. Syst. Ind. Manag. Appl.*, vol. 8, pp. 205–213, 2016. [Online]. Available: http://www.mirlabs.org/ijcisim/regular_papers_2016/IJCISIM_21.pdf

[3] X. Huang, T. Han, and N. Ansari, “On green energy powered cognitive radio networks”, *IEEE Communications Surveys and Tutorials*, vol. 17, no. 2, pp. 827–842, 2015. DOI: 10.1109/COMST.2014.2387697.

[4] A. Bhowmick, K. Yadav, S. D. Roy, and S. Kundu, “Throughput of an energy harvesting cognitive radio network based on prediction of primary user”, *IEEE Trans. Veh. Technol*., vol. 66, no. 9, pp. 8119–8128, 2017. DOI: 10.1109/TVT.2017.2690675.

[5] M.-L. Ku, W. Li, Y. Chen, and K. J. Ray Liu, “Advances in energy harvesting communications: Past, present, and future challenges”, *IEEE Commun. Surv. Tutorials*, vol. 18, no. 2, pp. 1384–1412, 2016. DOI: 10.1109/COMST.2015.2497324.

[6] S. Park, H. Kim, and D. Hong, “Cognitive radio networks with energy harvesting”, *IEEE Trans. Wirel. Commun*., vol. 12, no. 3, pp. 1386–1397, 2013. DOI: 10.1109/TWC.2013.012413.121009.

[7] S. Park and D. Hong, “Optimal spectrum access for energy harvesting cognitive radio networks”, *IEEE Trans. Wirel. Commun*., vol. 12, no. 12, pp. 6166–6179, 2013. DOI: 10.1109/TWC.2013.103113.130018.

[8] A. Alsharoa, N. Neihart, S. W. Kim, and A. E. Kamal, “Multi-band RF energy and spectrum harvesting in cognitive radio networks”, in *Proc. of 2018 IEEE International Conference on Communications (ICC)*, 2018, pp. 1–6. DOI: 10.1109/ICC.2018.8422511.

[9] F. Zhang, T. Jing, Y. Huo, and K. Jiang, “Throughput maximization for energy harvesting cognitive radio networks with finite horizon”, in *Proc. of 2017 9th International Conference on Wireless Communications and Signal Processing (WCSP)*, 2017, pp. 1–7. DOI: 10.1109/WCSP.2017.8171190.

[10] W. Chung, S. Park, S. Lim, and D. Hong, “Spectrum sensing optimization for energy-harvesting cognitive radio systems”, *IEEE Trans. Wirel. Commun.*, vol. 13, no. 5, pp. 2601–2613, 2014. DOI: 10.1109/TWC.2014.032514.130637.

[11] Z. Li, B.-Y. Liu, J.-B. Si, and F.-H. Zhou, “Optimal satisfaction degree in energy harvesting cognitive radio networks”, *Chinese Phys. B*, vol. 24, no. 12, art. ID 128401, 2015. DOI: 10.1088/1674-1056/24/12/128401.

[12] S. Zhang, H. Zhao, A. S. Hafid, and S. Wang, “Joint optimization of energy harvesting and spectrum sensing for energy harvesting cognitive radio”, in *Proc. of 2016 IEEE 84th Vehicular Technology Conference (VTC-Fall)*, 2016, pp 1–5. DOI: 10.1109/VTCFall.2016.7881058.

[13] J. Elhachmi and Z. Guennoun, “Cognitive radio spectrum allocation using genetic algorithm”, *Eurasip J. Wirel. Commun. Netw.*, vol. 2016, art. no. 133, 2016. DOI: 10.1186/s13638-016-0620-6.

[14] Z. Zhao, S. Yin, L. Li, and S. Li, “Optimal-stopping spectrum Sensing in energy harvesting cognitive radio systems”, *Journal of Signal Processing Systems*, vol. 90, pp. 807–825, 2018. DOI: 10.1007/s11265-018-1342-2.

[15] Y. Pei, Y.-C. Liang, K. C. Teh, and K. H. Li, “Sensing-throughput tradeoff for cognitive radio networks: A multiple-channel scenario”, in *Proc. of 2009 IEEE 20th International Symposium on Personal, Indoor and Mobile Radio Communications*, 2009, pp. 1257–1261. DOI: 10.1109/PIMRC.2009.5450216.

[16] L. Luo and S. Roy, “Efficient spectrum sensing for cognitive radio networks via joint optimization of sensing threshold and duration”, *IEEE Trans. Commun.*, vol. 60, no. 10, pp. 2851–2860, 2012. DOI: 10.1109/TCOMM.2012.072612.100605.

[17] H. Hu, H. Zhang, J. Guo, and F. Wang, “Joint optimization of sensing and power allocation in energy-harvesting cognitive radio networks”, *ACM Trans. Embed. Comput. Syst.*, vol. 17, no. 1, art. no. 8, pp. 1–21, 2018. DOI: 10.1145/3070709.

[18] Z. Li, B. Liu, J. Si, and F. Zhou, “Optimal spectrum sensing interval in energy-harvesting cognitive radio networks”, *IEEE Trans. Cogn. Commun. Netw.*, vol. 3, no. 2, pp. 190–200, 2017. DOI: 10.1109/TCCN.2017.2702167.

[19] K. Zheng, X. Liu, Y. Zhu, K. Chi, and K. Liu, “Total throughput maximization of cooperative cognitive radio networks with energy

harvesting", *IEEE Trans. Wirel. Commun.*, vol. 19, no. 1, pp. 533–546, 2020. DOI: 10.1109/TWC.2019.2946813.

[20] I. S. Abdelfattah, S. I. Rabia, and A. M. Abdelrazek, "Optimal sensing energy and sensing interval in cognitive radio networks with energy harvesting", *Int. J. Commun. Syst.*, vol. 34, no. 7, p. e4742, 2021. DOI: 10.1002/dac.4742.

[21] S. Chatterjee, S. P. Maity, and T. Acharya, "Energy-spectrum efficiency trade-off in energy harvesting cooperative cognitive radio networks", *IEEE Trans. Cogn. Commun. Netw.*, vol. 5, no. 2, pp. 295–303, 2019. DOI: 10.1109/TCCN.2019.2903503.

[22] S. Yin, Z. Qu, and S. Li, "Achievable throughput optimization in energy harvesting cognitive radio systems", *IEEE Journal on Selected Areas in Communications*, vol. 33, no. 3, pp. 407–422, 2015. DOI: 10.1109/JSAC.2015.2391712.

[23] A. Balieiro, P. Yoshioka, K. Dias, D. Cavalcanti, and C. Cordeiro, "A multi-objective genetic optimization for spectrum sensing in cognitive radio", *Expert Syst. Appl.*, vol. 41, no. 8, pp. 3640–3650, 2014. DOI: 10.1016/j.eswa.2013.12.010.

[24] P. M. Pradhan and G. Panda, "Comparative performance analysis of evolutionary algorithm based parameter optimization in cognitive radio engine: A survey", *Ad Hoc Networks*, vol. 17, pp. 129–146, 2014. DOI: 10.1016/j.adhoc.2014.01.010.

[25] R. Han, Y. Gao, C. Wu, and D. Lu, "An effective multi-objective optimization algorithm for spectrum allocations in the cognitive-radio-based Internet of Things", *IEEE Access*, vol. 6, pp. 12858–12867, 2018. DOI: 10.1109/ACCESS.2017.2789198.

[26] Md S. Miah, M. Schukat, and E. Barrett, "A throughput analysis of an energy-efficient spectrum sensing scheme for the cognitive radio-based Internet of things", *EURASIP Journal on Wireless Communications and Networking*, vol. 2021, no. 1, 2021. DOI: 10.1186/s13638-021-02075-2.

[27] C. A. C. Coello, G. T. Pulido, and M. S. Lechuga, "Handling multiple objectives with particle swarm optimization", *IEEE Trans. on Evolutionary Comput*., vol. 8, no. 3, pp. 256–279, Jun. 2004. DOI: 10.1109/TEVC.2004.826067.

[28] Vikas and S. J. Nanda, "Multiobjective Moth Flame Optimization", in *Proc. of 2016 International Conference on Advances in Computing, Communications and Informatics (ICACCI)*, 2016, pp. 2470–2476. DOI: 10.1109/ICACCI.2016.7732428.

[29] S. Mirjalili, P. Jangir, and S. Saremi, "Multiobjective ant lion optimizer: A multiobjective optimization algorithm for solving engineering problems", *Appl. Intell.*, vol. 46, no. 1, pp. 79–95, 2016. DOI: 10.1007/s10489-016-0825-8.

[30] L. Du and C. Huang, "Save-then-transmit scheme for fading channels with random energy harvesters", in *Proc. of 2017 23rd Asia-Pacific Conf. Commun. (APCC)*, 2017, pp. 1–6. DOI: 10.23919/APCC.2017.8304076.

[31] Y. Chen, *Energy Harvesting Communications: Principles and Theories*. Coventry, UK: John Wiley & Sons, 2019. DOI: 10.1002/9781119383062.

[32] A. Sultan, "Sensing and transmit energy optimization for an energy harvesting cognitive radio", *IEEE Wirel. Commun. Lett.*, vol. 1, no. 5, pp. 500–503, 2012. DOI: 10.1109/WCL.2012.071612.120304.

[33] S. Mirjalili, "Moth-flame optimization algorithm: A novel nature inspired heuristic paradigm", *Knowledge-Based Systems*, vol. 89, pp. 228–249, 2015. DOI: 10.1016/j.knosys.2015.07.006.

[34] I. Scharf, A. Subach, and O. Ovadia, "Foraging behaviour and habitat selection in pit-building antlion larvae in constant light or dark conditions", *Anim. Behav.*, vol. 76, no. 6, pp. 2049–2057, 2008. DOI: 10.1016/j.anbehav.2008.08.023.

[35] S. Mirjalili, "The ant lion optimizer", *Adv. Eng. Softw.*, vol. 83, pp. 80–98, 2015. DOI: 10.1016/j.advengsoft.2015.01.010.

[36] H. Kılıç and U. Yüzgeç, "Tournament selection based antlion optimization algorithm for solving quadratic assignment problem", *Eng. Sci. Technol., Int. J.*, vol. 22, no. 2, pp. 673–691, 2019. DOI: 10.1016/j.jestch.2018.11.013.

[37] G. Eappen and T. Shankar, "Hybrid PSO-GSA for energy efficient spectrum sensing in cognitive radio network", *Phys. Commun.*, vol. 40, art. 101091, 2020. DOI: 10.1016/j.phycom.2020.101091.

[38] X. Lu, P. Wang, D. Niyato, and E. Hossain, "Dynamic spectrum access in cognitive radio networks with RF energy harvesting", *IEEE Wirel. Commun.*, vol. 21, no. 3, pp. 102–110, 2014. DOI: 10.1109/MWC.2014.6845054.

[39] S. Mirjalili, "Dragonfly algorithm: A new meta-heuristic optimization technique for solving single-objective, discrete, and multiobjective problems", *Neural Comput. & Applications*, vol. 27, pp. 1053–1073, 2016. DOI: 10.1007/s00521-015-1920-1.

[40] M. Jamil and X.-S. Yang, "A literature survey of benchmark functions for global optimization problems", *International Journal of Mathematical modelling and Numerical Optimization*, vol. 4, no. 2, pp. 150–194, 2013. DOI: 10.1504/IJMMNO.2013.055204.

[41] P. Kumar and A. Bhowmick, "Throughput performance of a non-linear energy-harvesting cognitive radio-enabled device-to-device network", *Int. J. Communication Syst.*, vol. 35, no. 9, p. e5124, 2022. DOI: 10.1002/dac.5124.

[42] C. Salto and E. Alba, "Cellular genetic algorithms: Understanding the behavior of using neighborhoods", *Appl. Artif. Intell.*, vol. 33, no. 10, pp. 863–880, 2019. DOI: 10.1080/08839514.2019.1646005.

[43] M. K. Hasan, Md. M. J. Chowdhury, S. Ahmed, S. R. Sabuj, J. Nibhen, and K. A. A. Bakar, "Optimum energy harvesting model for bidirectional cognitive radio networks", *Eurasip J. Wirel. Commun. Netw.*, vol. 2021, art. no. 199, 2021. DOI: 10.1186/s13638-021-02064-5.